Water-Dispersible Conducting Polyaniline/Nano-SiO_2 Composites without Any Stabilizer

Xingwei Li, Na Dai, Gengchao Wang, Xiaomei Song

Key Laboratory for Ultrafine Materials of Ministry of Education, School of Material Science and Engineering, East China University of Science and Technology, Shanghai 200237, People's Republic of China

Received 27 October 2006; accepted 3 June 2007
DOI 10.1002/app.27074
Published online 20 September 2007 in Wiley InterScience (www.interscience.wiley.com).

ABSTRACT: A water-dispersible conducting polyaniline/nano-SiO_2 composite, with a conductivity of 0.071 S cm^{-1} at 25°C, was prepared by the oxidative polymerization of aniline in the presence of amorphous nano-SiO_2 particles. And the structure, morphology, thermal stability, conductivity, and electroactivity of this composite were also investigated. This composite has been steadily dispersed in the aqueous solution for about 10–36 h without the need for any stabilizer. It would significantly impulse the commercial applications of conducting polyaniline/nano-SiO_2 composite as fillers for antistatic and anticorrosion coatings. © 2007 Wiley Periodicals, Inc. J Appl Polym Sci 107: 403–408, 2008

Key words: polyaniline; nano-SiO_2; composite; conductivity; dispersibility

INTRODUCTION

Low cost, good environmental stability and high electrical conductivity make polyaniline (PAni) become one of the most attractive conducting polymers.[1–5] However, conducting PAni is difficult to be processed through traditional methods as most conducting polymers are. Therefore, many potential applications of PAni still remain unexploited. To solve the problem of processability, synthesis techniques have been found and optimized to incorporate the inorganic component into the conducting PAni matrix. Recently, conducting PAni/inorganic nanocomposites have also attracted more and more attention. A number of different metals and metal oxide particles have so far been encapsulated into the shell of conducting PAni to produce a host of nanocomposites. These composite materials have shown better mechanical, physical and chemical properties, due to combining the merits of conducting PAni and inorganic nanoparticles. And their properties can be easily adjusted to meet the desired applications via the variation of particle size, shape and the distribution of nanoparticles. Therefore, they have wide potential applications in diverse areas such as chemistry, physics, electronic, optics, materials, and biomedical science.[6–12]

Among those inorganic nanoparticles, nano-SiO_2 particles are appealing because of their excellent reinforcing properties for polymer materials.[13,14] However, nano-SiO_2 is an insulator. To expand the applications of insulator nano-SiO_2 as fillers and improve the processability of PAni, many works have been done. Several papers on PAni/nano-SiO_2 composite have been published.[15–22] For instance, Gill et al.[15] characterized a new PAni-silica composite colloid by various particle sizing techniques. Their studies have confirmed that these composite particles consist of submicronic aggregates of the original small silica particles held together by the PAni ''binder,'' resulting in an unusual ''raspberry'' morphology. And Stejskal et al.[16] prepared a PAni dispersions in the presence of ultrafine colloidal silica. They founded that stable PAni-silica particles colloid in the range of 300–600 nm could be obtained, given a sufficient silica concentration. The electrical conductivity of the PAni(37.8 wt %)-silica composite is 0.06 S cm^{-1} at 25°C. Ita et al.[20] obtained PAni/silica hybrid gel by chemical polymerization of aniline in the sol-gel systems of tetramethoxysilane using ammonium peroxodisulfate as initiator and sodium dodecyl sulfate as stabilizer. Our group had prepared PAni/nano-SiO_2 composite by surface modification of partly crystalline nano-SiO_2 using PAni. This composite only contained 15% PAni, and its conductivity had reached 0.32 S cm^{-1} at 25°C.[23] However, it is to be regretted that this composite is unable to disperse stably in aqueous solution after stopping ultrasonic action.

Correspondence to: X. Li (lixingwei_nj@yahoo.com).
Contract grant sponsor: Key Programs of Ministry of Education of China; contract grant number: No106074.
Contract grant sponsor: Key Laboratory for Ultrafine Materials, Ministry of Education.

Journal of Applied Polymer Science, Vol. 107, 403–408 (2008)

Recently, we founded that amorphous nano-SiO_2 particles are more easily dispersed in aqueous solution than partly crystalline nano-SiO_2 particles. Herein, a simple approach to synthesize water-dispersible conducting PAni/nano-SiO_2 composite was reported. This composite was successfully prepared by the oxidative polymerization of aniline in the presence of amorphous nano-SiO_2 particles. It was believed that the obtained PAni/nano-SiO_2 composite particles were coated by an overlay of nano-SiO_2 particles with hydrophilic surfaces provided that there was a sufficient excess of nano-SiO_2 particles in the reaction system.[16] Small sized and negatively charged nano-SiO_2 particles produce the most effective stabilization by both the well-known charge stabilization mechanism and steric effects. This composite, with a conductivity of 0.071 S cm^{-1} at 25°C, is easily dispersed in aqueous solution, and the resulting suspensions have been stable for about 10–36 h without any stabilizer. Water dispersions of PAni/nano-SiO_2 composite have two distinct advantages for applications including: (1) the simple formation of films by drop casting, the surface resistance of polyvinyl alcohol film (about 0.6 μm) added 3% PAni/nano-SiO_2 composite has descended from 5.0×10^{10} Ω to 1.4×10^5 Ω in our studies. And (2) it is more environmentally benign processing than that with organic solvents.

EXPERIMENTAL

Materials

Aniline (Shanghai Chemical Works, China) was used after twice distillation. Nano-SiO_2 with an average particle size of ~ 20 nm (Jiang Su Hehai Nano-ST Company, China) was used without further purification. Other chemicals were of AR grade. De-ionized water was used in this investigation.

Syntheses of conducting PAni/nano-SiO_2 composite and control PAni

PAni/nano-SiO_2 composite was prepared as the following. Aniline (1 mL) was injected to 70 mL of 2*M* HCl containing 1 g nano-SiO_2 particles under ultrasonication to break the aggregation of nano-SiO_2 particles. After 1 h, 2.5 g $(NH_4)_2S_2O_8$ (dissolved in 20 mL de-ionized water) was added drop-wise into the above solution while stirring was applied constantly. The polymerization was allowed to proceed for 5 h at room temperature. The solid product was obtained by filtration, then washed with 2*M* HCl and de-ionized water to remove residual aniline hydrochloride and ammonium sulfate. Finally, it was dried at 60°C for 24 h under vacuum. The final product was a fine tint green powder.

Control PAni was prepared as above but without the nano-SiO_2, and obtained a fine dark green powder.

Characterization

Fourier-transform infrared spectra (FTIR) of the powder samples were recorded with a Nicolet Magna-IR550 spectrometer. Measurements were performed in the transmission mode in KBr pellets.

UV-vis spectra of the samples were recorded on a VARIAN Cary 500 UV-vis spectrophotometer. Samples (0.001 g) were dispersed in 10 mL de-ionized water under ultrasonic action.

Fully corrected fluorescence spectra were recorded on a Fluorolog-3 luminescence spectrophotometer from Jobin Yvon. Samples were dispersed in de-ionized water under ultrasonication. The excitation wavelength was 290nm.

Measurements of wide-angle X-ray diffraction (WXRD) were taken on a Rigaku D/Max 2550 VB/PC X-ray diffractometer using CuK_α radiation ($\lambda = 0.154$ nm).

Thermogravimetric analysis was performed on a Shimadzu TGA-50 instrument at the heating rate of 10°C min^{-1} in air.

The sample morphology was observed by using a JEM-100S transmission electron microscopy.

Conductivity was measured on compressed pellet of the powder sample by using the conventional four-probe technique at 25°C.

Cyclic voltammograms of PAni and PAni/nano-SiO_2 composite were studied in a one-compartment three-electrode cell using a custom-built potentiostat connected to a computer with an AD/DA converter. To measure the cyclic voltammetry, PAni or PAni/SiO_2 composite (0.05 g) was suspended in 20 mL de-ionized water and sonificated for several minutes. A few drops of this suspension were carefully transferred to the surface of working electrode (Pt sheet of 2 mm diameter). After water evaporation (at room temperature) a uniform film was formed, then was rinsed with de-ionized water. A Pt sheet and a saturated calomel electrode (SCE) were used as the counter and reference electrodes, respectively. CVs were recorded in 0.1*M* H_2SO_4. The scan speed was 50 mV/s and the potential ranged from −200 mV–1000 mV.

The surface resistance of polyvinyl alcohol film was measured using a ZC46A high ohmmeter.

RESULTS AND DISCUSSIONS

Morphology of PAni/nano-SiO_2 composite and aqueous colloids

TEM of Nano-SiO_2, PAni and PAni/nano-SiO_2 composite were shown in Figure 1, respectively.

Aggregation, a common yet complex phenomenon for small particles, is problematic in the production and the use of nanostructured materials. Aggregation makes nanostructured materials especially be difficult to explore the properties and applications. Figure 1(a) showed that morphology of PAni was different from that of nano-SiO_2 and PAni/nano-SiO_2 composite, and it was aggregated in aqueous solution with an irregular shape. And nano-SiO_2 and PAni/nano-SiO_2 composite were nearly spherical in shape. Comparing with PAni and nano-SiO_2, PAni/nano-SiO_2 composite was more easily dispersed in aqueous solution, and films could be readily fabricated from colloidal dispersions through casting, as shown in Figure 1(d). This result was also supported by the fact that it only took 5 min to disperse PAni/nano-SiO_2 composite under ultrasonic action, and the resulting suspensions were stable about 10–36 h after ultrasonic dispersion. The surface resistance of polyvinyl alcohol film (about 0.6 μm) added 3% PAni/nano-SiO_2 composite has descended from 5.0×10^{10} Ω to 1.4×10^5 Ω. But it took about 30 min to disperse PAni, and that suspension of PAni could only be stable for about 5–10 min after ultrasonic dispersion.

Conductivity and cyclic voltammograms

The conductivity of PAni/nano-SiO_2 composite containing 45% conducting PAni is 0.071 S cm^{-1} at 25°C. Although its conductivity reduces two orders of magnitude in comparison with that of control PAni (2.75 S cm^{-1}), it is still useful to expand the applications of nano-SiO_2 and improve the processability of PAni.

Cyclic voltammetry (CV) of PAni and PAni/nano-SiO_2 composite was performed in 0.1*M* H_2SO_4, and CVs were shown in Figure 2. From Figure 2(a), it was seen that the coatings of PAni deposited on the Pt electrodes showed two pairs of redox characteristics, but with low definition in comparison with the ones synthesized electrochemically in aqueous acids.[24] Figure 2(b) suggested that electroactivity of PAni/nano-SiO_2 composite was from PAni layer. However, redox reversibility of PAni in PAni/nano-SiO_2 composite was poorer than that of control PAni. This should be due to the presence of nano-SiO_2 particles, which diminished the extent of conjugation of PAni macromolecules.[9]

Thermal stability

Figure 3 illustrates the results of thermogravimetric analysis of PAni/nano-SiO_2 composite and PAni.

Nano-SiO_2 particles are very stable in air and almost no decomposition takes place in the range of 20 ~ 800°C, and only gives a small weight loss in the range of low temperature, which is presumably the water content of nano-SiO_2 substrate.

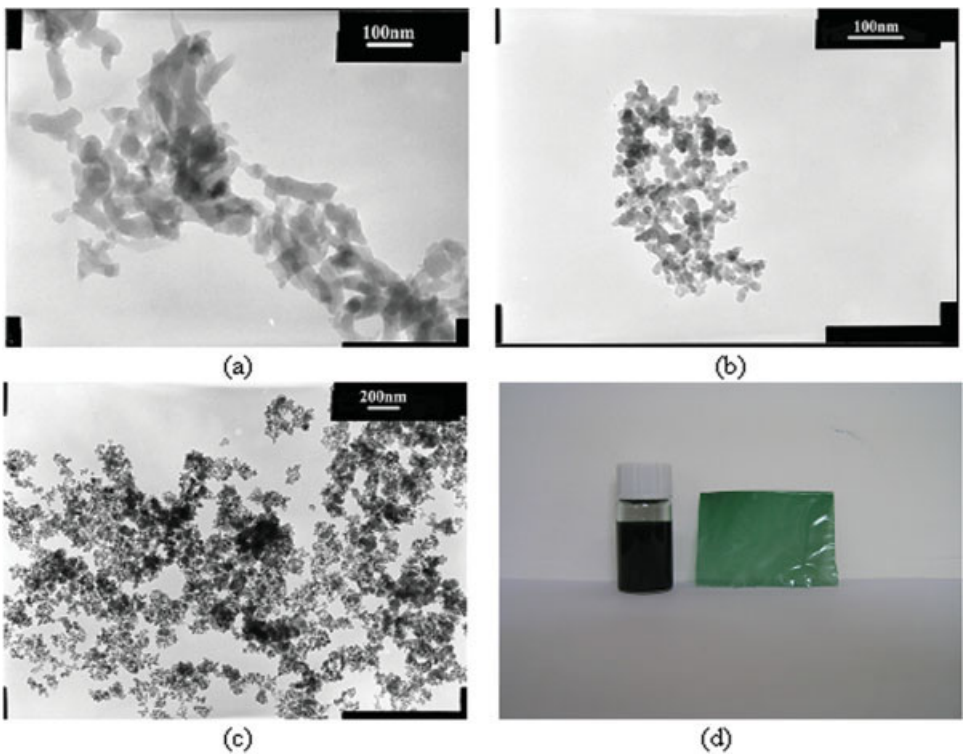

Figure 1 TEM of PAni (a), TEM of Nano-SiO_2 (b), TEM of PAni/nano-SiO_2 composite (c) and PAni/nano-SiO_2 composite aqueous colloids (24 h after stopping the ultrasonic action) (d). [Color figure can be viewed in the online issue, which is available at www.interscience.wiley.com]

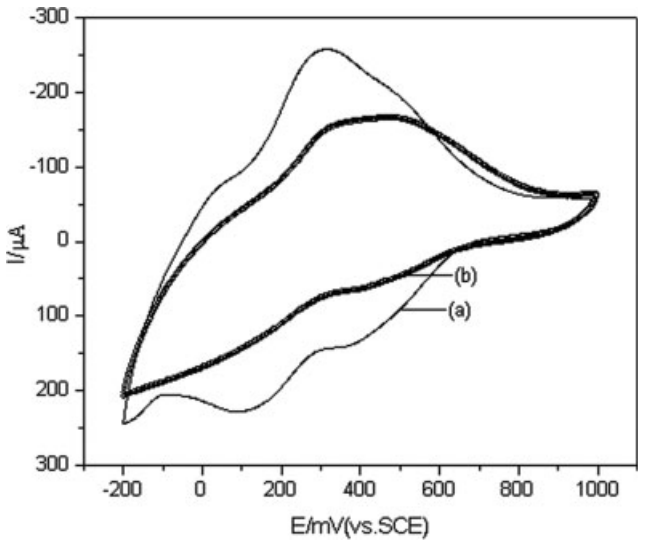

Figure 2 Cyclic voltammograms of PAni (a) and PAni/nano-SiO_2 composite (b) Electrolytic solution: 0.1*M* H_2SO_4, Sweep rate: 50 mV/s.

From curve-b in Figure 3, it can be seen that thermal degradation of PAni occurs at 389°C. The initial mass loss at lower temperatures is mainly due to the release of water and dopant anions from the PAni. A sharp loss in mass is possibly due to a large scale of thermal degradation of the PAni chains. Curve-a shows that the temperature of thermal decomposition of PAni/nano-SiO_2 composite is about 343°C, which is lower than that of control PAni. The drop in temperature would be explained by the fact that an interaction at the interface of nano-SiO_2 and PAni weakens the force of PAni interchains, and makes for thermal decomposition of PAni in this composite. PAni/nano-SiO_2 composite exhibits a PAni layer mass of 45% in comparison with Curve-a and Curve-b in Figure 3.

Fourier transform infrared spectra

FTIR spectra of nano-SiO_2, PAni/nano-SiO_2 composite and control PAni are shown in Figure 4, respectively. The main characteristic peaks of PAni are assigned as the following. The peaks at 1569 cm^{-1} and 1476 cm^{-1} are attributable to C=N and C=C stretching modes for the quinoid and benzenoid rings, and the peaks at 1297 cm^{-1} and 1229 cm^{-1} are attributed to C—N stretching mode for benzenoid ring, while the peak at 1127 cm^{-1} is assigned to a plane bending vibration of C—H, which is formed during protonation.[25] It is also noted, by comparing Figure 4(a) with Figure 4(b), that some peaks of PAni are shifted due to the presence of nano-SiO_2 particles. For example, the peaks at 1569 cm^{-1}, 1476 cm^{-1}, 1297 cm^{-1}, and 1229 cm^{-1} shift to higher wavenumbers, and the peak at 1127 cm^{-1} shift to lower wavenumbers. These changes also suggest that an interaction exists between PAni macromolecule and nano-SiO_2 particles. This interaction is highly likely the hydrogen bonding between the surfaces of the electronegative nano-SiO_2 particles and the N—H group in PAni macromolecule.[26]

UV-vis absorption spectra

Figure 5 gives UV-vis absorption spectra of PAni and PAni/nano-SiO_2 composite. Nano-SiO_2 shows strong absorbance in the range of 200–300 nm, but the characteristic peaks do not appear. Conse-

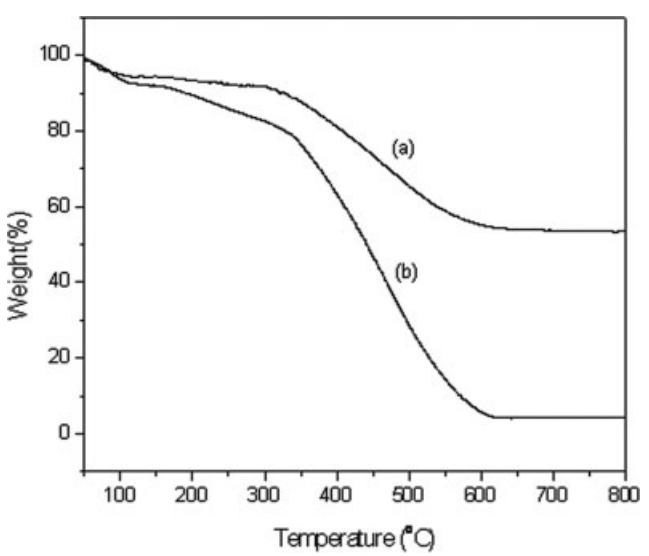

Figure 3 TGA of PAni/nano-SiO_2 composite (a) and PAni (b).

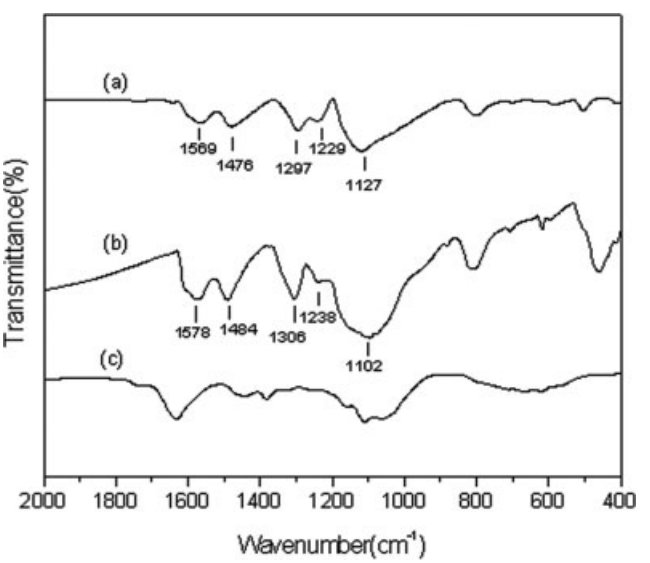

Figure 4 FTIR of PAni (a), PAni/nano-SiO_2 composite (b) and nano-SiO_2 (c).

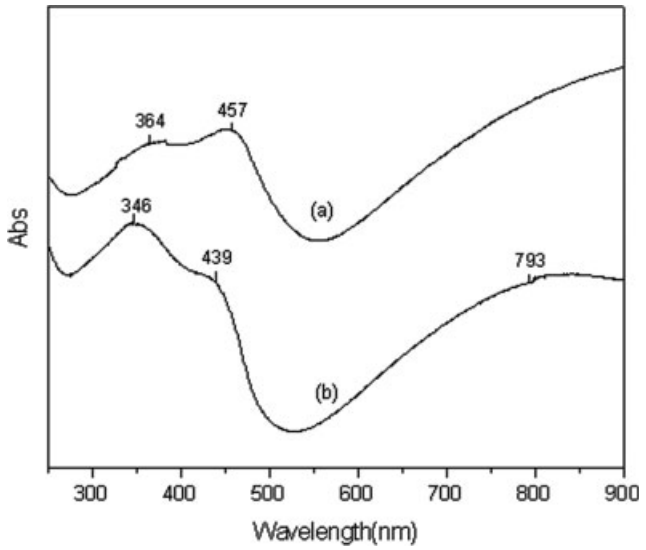

Figure 5 UV-vis absorption spectra of PAni (a) and PAni/nano-SiO_2 composite (b).

quently, UV-vis spectrum of nano-SiO_2 is not illustrated.

Figure 5(a) indicates that PAni has three characteristic peaks, which are at 364 nm, 457 nm, and around 900 nm. The peak at 364 nm arises from electron transition within the benzenoid segments, while the absorption peaks at 457 nm and around 900 nm originate from the charged cationic species known as polarons.[21,27]

From Figure 5(b), it can be seen that all characteristic peaks shift to shorter wavelengths in PAni/nano-SiO_2 composite, and the intensity ratios of the peak at 364 nm to the peaks at 457 nm and at around 900 nm are also changed. This implies that

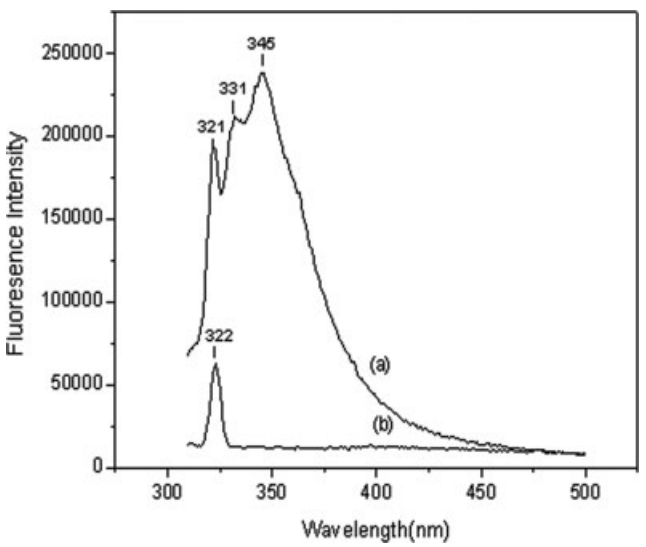

Figure 6 Fluorescence emission spectra of PAni (a) and PAni/nano-SiO_2 composite (b).

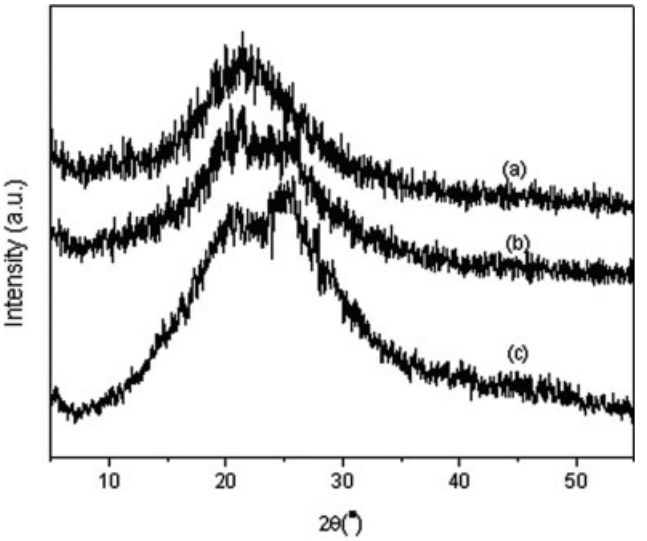

Figure 7 WXRD of nano-SiO_2 (a), PAni/nano-SiO_2 composite (b) and PAni(c).

the presence of nano-SiO_2 has also an effect on the doping level of conducting PAni, which arises from an interaction between PAni macromolecule and nano-SiO_2 particles.

Fluorescence

The fluorescence emission spectra of PAni and PAni/nano-SiO_2 composite are displayed in Figure 6. Figure 6 shows that the presence of nano-SiO_2 results in the changes of fluorescence spectra of PAni. The peaks at 331 nm and 345 nm disappear in PAni/nano-SiO_2 composite. It means that presence of nano-SiO_2 particles influences the conjugate electrons conformation of PAni. The interaction between nano-SiO_2 and PAni decreases the degree of orbital overlapping between π electrons of phenyl rings with the lone pair of nitrogen atom. Consequently, the extent of conjugation of PAni diminishes.

WXRD patterns

WXRD patterns of Nano-SiO_2, PAni and PAni/nano-SiO_2 composite are given in Figure 7. Figure 7 shows that there are two broad peaks center at $2\theta = 20.4^\circ$ and 25.2° in PAni macromolecule, which are ascribed to the periodicity parallel and perpendicular to the polymer chains of PAni, respectively.[28] Figure 7(b) suggests that the presence of amorphous nano-SiO_2 does not affect on the crystallinity of PAni, though it improved the processability of PAni.

CONCLUSIONS

A water-dispersible conducting PAni/nano-SiO_2 composite was successfully prepared by the oxida-

tive polymerization of aniline in the presence of amorphous nano-SiO_2 particles. The method we employed was very simple and inexpensive in comparison with methods applied by other researchers, and it can be easily applied to industrialization. This composite, whose conductivity is 0.071 S cm^{-1} at 25°C, can be steadily dispersed in the aqueous solution for about 10–36 h without any stabilizer. It is hopeful to be used in commercial applications as environmental protection fillers for antistatic and anticorrosion coatings.

References

1. MacDiarmid, A. G. Angew Chem Int Ed 2001, 40, 2581.
2. Huang, J. X.; Kaner, R. B. J Am Chem Soc 2004, 126, 851.
3. Chiou, N. R.; Epstein, A. J. Adv Mater 2005, 17, 1679.
4. Shreepathi, S.; Holze, R. Chem Mater 2005, 17, 4078.
5. Huang, J. X. Pure Appl Chem 2006, 78, 15.
6. Gangopadhyay, R.; De, A. Chem Mater 2000, 12, 608.
7. Schnitzler, D. C.; Meruvia, M. S.; Hümmelgen, I. A.; Zarbin, A. J. G. Chem Mater 2003, 15, 4658.
8. Zeng, C. C.; Han, X. M.; Lee, L. J.; Koelling, K. W.; Tomasko, D. L. Adv Mater 2003, 15, 1743.
9. Schnitzler, D. C.; Zarbin, A. J. G. J Braz Chem Soc 2004, 15, 378.
10. Majumdar, G.; Goswami, M.; Sarma, T. K.; Paul, A.; Chattopadhyay, A. Langmuir 2005, 21, 1663.
11. Chowdhury, D.; Paul, A.; Chattopadhyay, A. Langmuir 2005, 21, 4123.
12. Feng, X. M.; Yang, G.; Xu, Q.; Hou, W. H.; Zhu, J. J. Macromol Rapid Commun 2006, 27, 31.
13. Hasan, M. M.; Zhou, Y.; Mahfuz, H.; Jeelani, S. Mater Sci Eng A 2006, 429, 181.
14. Yu, T. S.; Lin, J. P.; Xu, J. F.; Ding, W. W. J Polym Sci Part B: Polym Phys 2005, 43, 3127.
15. Gill, M.; Armes, S. P.; Fairhurst, D.; Emmett, S. N.; Idzorek, G.; Pigottt, T. Langmuir 1992, 8, 2178.
16. Stejskal, J.; Kratochvı´l, P.; Armes, S. P.; Lascelles, S. F.; Riede, A.; Helmstedt, M.; J. Prokeš; Křivka, I. Macromolecules 1996, 29, 6814.
17. Riede, A.; Helmstedt, M.; Riede, V.; Zemek, J.; Stejskal, J. Langmuir 2000, 16, 6240.
18. Stejskal, J. J Polym Mater 2001, 18, 225.
19. Wang, Y.; Wang, X. H.; Li, J.; Mo, Z. S.; Zhao, X. J.; Jing, X. B.; Wang, F. S. Adv Mater 2001, 13, 1582.
20. Ita, M.; Uchida, Y.; Matsui, K. J Sol-Gel Sci Technol 2003, 26, 479.
21. Xia, H. S.; Wang, Q. J Appl Polym Sci 2003, 87, 1811.
22. Stejskal, J.; Trchova, M.; Fedorova, S.; Sapurina, I.; Zemek, J. Langmuir 2003, 19, 3013.
23. Li, X. W.; Wang, G. C.; Li, X. X. Surface Coat Technol 2005, 197, 56.
24. Lapkowski, M.; Berrada, K.; Quillard, S.; Louran, G.; Lefrant, S.; Pron, A. Macromolecules 1995, 28, 1223.
25. Kang, E. T.; Neho, K. G.; Tan, K. L. Prog Polym Sci 1998, 23, 277.
26. Niu, Z. W.; Yang, Z. Z.; Hu, Z. B.; Lu, Y. F.; Han, C. C. Adv Funct Mater 2003, 13, 949.
27. Zhang, L. J.; Wang, M. X. J Phys Chem B 2003, 107, 6748.
28. Zhang, Z. M.; Wei, Z. X.; Wan, M. X. Macromolecules 2002, 35, 5937.